Solar Radiation Assisted Natural Convection in Uniform Porous Medium Supported by a Vertical Flat Plate

A. J. Chamkha
Department of Mechanical and Industrial Engineering, Kuwait University, P.O. Box 5969, Safat, 13060 Kuwait

Natural convection flow of an absorbing fluid up a uniform porous medium supported by a semi-infinite, ideally transparent, vertical flat plate due to solar radiation is considered. Boundary-layer equations are derived using the usual Boussinesq approximation and accounting for applied incident radiation flux. A convection type boundary condition is used at the plate surface. These equations exhibit no similarity solution. However, the local similarity method is employed for the solution of the present problem so as to allow comparisons with previously published work. The resulting approximate nonlinear ordinary differential equations are solved numerically by a standard implicit iterative finite-difference method. Graphical results for the velocity and temperature fields as well as the boundary friction and Nusselt number are presented and discussed.

Introduction

Natural convection flow in porous media supported by surfaces has application in a broad spectrum of engineering systems. Some of these include geothermal reservoirs, building thermal insulation, direct-contact heat exchangers, solar heating systems, packed-bed catalytic reactors, nuclear waste disposal systems, and enhanced recovery of petroleum resources. Most studies of natural convection in porous media have been based on Darcy's law which is applicable for slow flows and does not account for non-Darcian inertial effects. These effects represent the additional pressure drop across the porous media resulting from interpore mixing for fast flows. In this case, the total pressure drop across the porous medium is a quadratic function of the velocity of the fluid flowing in it. In the presence of a heated boundary, heat transfer to the porous medium can be accounted for by employing the conservation of energy law and Brinkman's extension of Darcy's law modified to include the thermal buoyancy effect. The boundary and inertia effects on convective flow and heat transfer were analyzed and discussed by Vafai and Tien (1981).

In natural convection, flows combine with solar radiation effects and the radiative heat transfer often becomes substantial, even at relatively low temperatures. This is because the rates of natural convection heat transfer are often small, as is the case in gases. Depending on the surface properties and geometry, radiative transport is often comparable to, or larger than, the convective heat transfer in many practical applications. It is, therefore, of great significance and interest to investigate its effects on the flow and heat transfer aspects. The book by Gebhart et al. (1988) provides more discussions on the various convection-radiation situations and summarizes some of the work done in that area. The problem discussed in the present work is that of steady, laminar, two-dimensional, free convection flow of an absorbing fluid up a vertical heated flat plate embedded in a uniform porosity transparent medium. Heating to the plate is supplied by the absorbing working fluid which receives incident rays of solar radiation. This type of flow has direct applications in furnaces, natural water bodies, flames and fires, crystal growth, environmental heat transfer, glass technology, solar ponds, nuclear accident containment, and solar energy collectors with direct solar collection using an absorbing fluid. Typical absorbing and emitting fluids are ammonia, carbon dioxide, and water. The book by Siegal and Howell (1981) discusses combined convection-radiation effects of nonabsorbing and nonemitting fluids such as air, inert gases, and nitrogen. Vafai and Ettefagh (1988) analyzed the radiative and conductive heat transfer characteristics of a waste package canister in the absence of natural convection. Natural convection from a heated plate has been studied by many investigators (see, for instance, Kierkus, 1968; Hassan and Mohamed, 1970; Sparrow and Gregg, 1956; Elsayed and Fathalah, 1979; and Fathalah and Elsayed, 1980). Cheng and Minkowycz (1977) considered boundary-layer free convection in the presence of a Darcian porous medium and were able to obtain similarity solution for the case of a constant wall temperature. Non-Darcian inertia effects on heat transfer were considered by Plumb and Huenfeld (1981), Evans and Plumb (1978), Vafai and Tien (1982), and Hong et al. (1987). Kim and Vafai (1989) studied, in detail, buoyancy-driven fluid flow and heat transfer about a vertical flat plate embedded in a porous medium for the cases of constant wall temperature and constant wall heat flux using the Brinkman-extended Darcy flow model. In addition, Evans and Plumb (1978) reported on the influence of medium inertia on natural convection from a vertical isothermal surface adjacent to a fluid-saturated porous medium. Other related works can be found in the papers by Singh and Tewari (1993), Nakayama et al. (1990), Chen et al. (1989) and Chen and Lin (1995). The present work represents a generalization of the problem discussed by Fathalah and Elsayed (1980) to include a uniform porous medium with Darcian and Forchheimer (non-Darcian) effects. The semi-infinite vertical flat plate is assumed to be nonreflecting, nonabsorbing, and ideally transparent. In addition, the transparent plate has no other thermal effects such as the axial thermal diffusion or thermal capacity. It is also assumed that the plate receives solar incident radiation flux which penetrates the plate and is absorbed by the fluid-saturated porous medium and that both the plate and the porous medium are in perfect thermal contact and are in local thermal equilibrium. By interaction with the absorbing fluid and the porous medium,

Contributed by the Heat Transfer Division for publication in the Journal of Heat Transfer. Manuscript received by the Heat Transfer Division December 4, 1995; revision received September 13, 1996; Keywords: Natural Convection, Porous Media, Radiation Interactions. Associate Technical Editor: K. Vafai.

both heat transfer from the fluid to the plate and heat loss from the plate to the surroundings take place. The fluid is assumed Newtonian, absorbing, and isotropic.

Mathematical Formulation

Consider steady, laminar, two-dimensional, free convection flow up a solar radiation-heated vertical semi-infinite flat plate immersed in a fluid-saturated porous medium. The coordinate system is such that x measures the distance along the plate and y measures the distance normally outward. The schematic of the problem under consideration is shown in Fig. 1. Both the surrounding and the absorbing fluid far away from the plate are maintained at a constant temperature T_∞. Due to the heating of the absorbing fluid and thus, the plate by radiation, heat is transferred from the plate to the surroundings. As mentioned before, the working fluid is assumed to be an absorbing one. In fact, one may have a nonabsorbing fluid. In this situation, the solid porous medium absorbs the incident solar radiation and transmits it to the working fluid by convection. Upon treating the fluid-saturated porous medium as a continuum (see Vafai and Tien, 1981), including the non-Darcian inertia effects, and assuming that the Boussinesq approximation is valid, the boundary-layer form of the governing equations can be written as (see Vafai and Tien, 1981; Gebhart et al., 1988)

$$\frac{\partial u}{\partial x} + \frac{\partial v}{\partial y} = 0 \tag{1}$$

$$u\frac{\partial u}{\partial x} + v\frac{\partial u}{\partial y} = \nu\frac{\partial^2 u}{\partial y^2} - \frac{\nu}{K}u - Cu^2 + g\beta(T - T_\infty) \tag{2}$$

$$u\frac{\partial T}{\partial x} + v\frac{\partial T}{\partial y} = \frac{k_e}{\rho c}\frac{\partial^2 T}{\partial y^2} + \frac{1}{\rho c}\frac{\partial q''_{\text{rad}}}{\partial y} \tag{3}$$

where u, v, and T are the fluid velocity components in the x and y direction, and the fluid temperature, respectively. ρ, ν, c, and k_e are the fluid density, kinematic viscosity, specific heat, and effective thermal conductivity, respectively. K and C are the porous medium permeability and inertia coefficient, respectively. g and β are the gravitational acceleration and coefficient of volumetric thermal expansion, respectively. q''_{rad} is the applied absorption radiation heat transfer per unit area. It should be noted that viscous dissipation is neglected and all properties are assumed constant except the density in the buoyancy term. In addition, the effect of porosity variation near the plate, and the dispersion effect, are negligible.

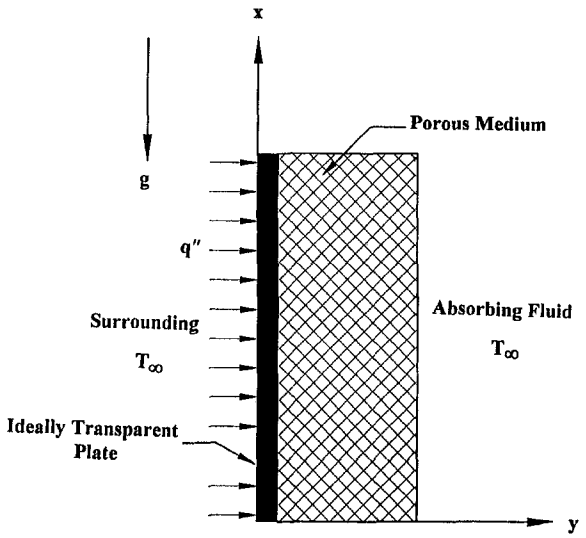

Fig. 1 Schematic of the problem

The appropriate boundary and matching conditions for the problem under consideration can be written as

$$u(x, 0) = 0, \quad v(x, 0) = 0,$$

$$k_e\frac{\partial T}{\partial y}(x, 0) = U(T(x, 0) - T_\infty) \quad u(x, \infty) = 0,$$

$$T(x, \infty) = T_\infty, \quad T(0, y) = T_\infty, \quad u(0, y) = 0 \quad (4a\text{--}g)$$

where U is the heat transfer coefficient for the heat lost from the plate to the surroundings; that is, the heat transfer coefficient between the inner surface of the plate and the ambient conditions. Equations $(4a, b)$ indicate that there is no slip condition and no suction or injection at the plate surface, respectively. Equation $(4c)$ indicates that the heat conduction at the plate is convected away to the surroundings. Equations $(4d, e)$ indicate that, far away from the plate, the fluid is undisturbed and is at the ambient or surrounding temperature. Equations $(4f, g)$

Nomenclature

a = absorption or extinction coefficient of fluid, m^{-1}
B_f = boundary friction, defined by Eq. $(14a)$
c = specific heat of fluid, J/kg K
C = porous medium inertia coefficient, m^{-1}
Da = Darcy number (Ka^2)
F = dimensionless stream function, defined by Eq. $(6g)$
g = gravitational acceleration, m/s^2
G = dimensionless normal velocity $(\partial F/\partial\xi)$
G_a = Grashof number based on absorption coefficient a, defined by Eq. $(6f)$
G_x = local Grashof number, defined by Eq. $(6e)$
h = heat transfer coefficient to the fluid, W/m^{2}K
H = dimensionless temperature gradient with ξ $(\partial\theta/\partial\xi)$
k_e = effective thermal conductivity of porous medium, W/mK
K = porous medium permeability, m^2
Nu_a = Nusselt number based on absorption coefficient a, defined by Eq. $(14b)$
Pr = effective Prandtl number, $(\mu c/k_e)$
q'' = incident radiation flux, W/m^2
q''_{rad} = radiation flux distribution in fluid, W/m^2, defined by Eq. (5)
T = dimensional fluid temperature, K
$T_{\max}$ = maximum local fluid temperature, K
T_w = wall or plate temperature, K
T_∞ = ambient temperature, K
u = dimensional tangential velocity, m/s
U = heat transfer loss coefficient to surroundings, W/m^{2}K
v = dimensional normal velocity, m/s
x, y = Cartesian coordinates along and normal to the plate, respectively, m
α = dimensionless heat transfer loss coefficient to surroundings $(U/(k_e a))$
β = volumetric expansion coefficient, K^{-1}
η = dimensionless normal distance defined by Eq. $(6d)$
Γ = dimensionless porous medium inertia coefficient (CG_a^5/a)
μ = dynamic viscosity of fluid, kg/ms
ν = kinematic viscosity of fluid, m^2/s
ρ = density of fluid, kg/m^3
ψ = stream function, m^2/s
θ = dimensionless temperature defined by Eq. $(6h)$
ξ = dimensionless tangential distance defined by Eq. $(6b)$

mean that the conditions at the plate's leading edge are such that the fluid is at a uniform temperature and stagnant.

Following Beer's law of radiation absorption as quoted by Cooper (1972) and Fathalah and Elsayed (1980), it will be assumed that

$$q''_{\text{rad}} = q''(1 - \exp(-ay)) \tag{5}$$

where q'' and a are the incident radiation flux (a constant) and the fluid's absorption or extinction coefficient (a constant), respectively. This law was applied to Dorsey's data for the absorption of radiation in water layers of different thicknesses. The estimated value of a ranges from 6 m^{-1} to 151.5 m^{-1} for distilled water of thickness 10 cm to 1 mm, respectively. The large variation in the values of a may be attributed to either inaccuracy of Dorsey's measurements, as stated by Cooper (1972), or to the reflectance and spectral dependence of the absorption coefficient of distilled water, which is not considered by Beer's law as stated by Fathalah and Elsayed (1980). In the present study, an absorption coefficient ranging between 200 m^{-1} and 2000 m^{-1} is assumed for a blackened grey water. The average value of radiation flux intensity q'' in Saudi Arabia and Kuwait is 900 w/m^2. It should be mentioned that it is assumed herein that the absorption of solar radiation and its distribution in the porous medium, which is made up of transparent solid material such as glass, occurs in the same manner as in a fluid. This may not be totally true since it is known that normally solid materials respond to radiation differently than a fluid, and that the mechanism of travel of its rays in solids is different than in a fluid. However, in general, it seems reasonable to assume that the form of Beer's law may be the same for a transparent solid-fluid system, but the values of the absorption coefficient will be different. In the presence of a porous solid material, the values of a will be higher than that of the fluid alone since the system will have higher energy capacity. This assumption is employed herein due to the absence of an experimentally based, proper form of solar energy distribution in a fluid-saturated porous medium, which is a solid-fluid combination, and as a first approximation. Numerical results for various values of a are reported subsequently. Therefore, the results of this work may be applied to such fluid-saturated transparent porous media that closely exhibit the behavior of Eq. (5). This highlights the need of extensive experimental effort in this area.

Equations (1) through (5) do not possess a similarity solution. However, the local nonsimilar technique employed by Sparrow and Yu (1971), and later by Fathalah and Elsayed (1980), appears to be suitable for this problem. This technique will be employed in this work. It is convenient to work with

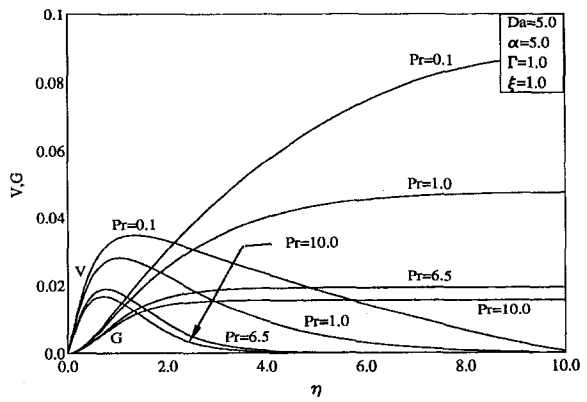

Fig. 2 Effects of Pr on tangential and normal velocity profiles

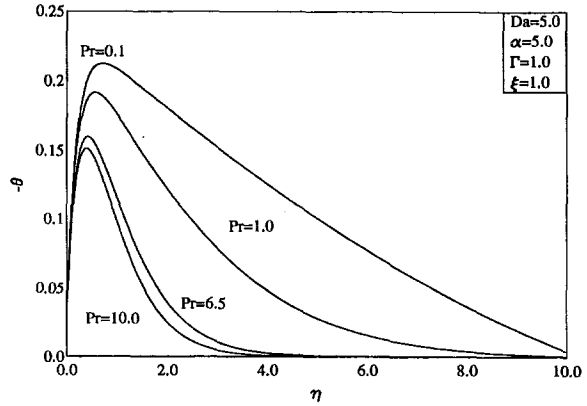

Fig. 3 Effects of Pr on temperature profiles

the stream function ψ and to nondimensionalize the governing equations by using the following transformations:

$$u = \frac{\partial \psi}{\partial y}, \quad v = -\frac{\partial \psi}{\partial x}, \quad \xi = \frac{G_x}{G_a^5}, \quad \eta = \frac{yG_x}{5x}$$

$$G_x = 5\left(\frac{g\beta q'' x^4}{5k_e\nu^2}\right)^{1/5}, \quad G_a = 5\left(\frac{g\beta q''}{5k_e\nu^2 a^4}\right)^{1/5}$$

$$\psi = \nu G_x F(\xi, \eta), \quad T = T_\infty - \frac{5xq''}{k_e G_x}\theta(\xi, \eta) \quad (6a\text{–}h)$$

where G_x is the local Grashof number based on the distance along the plate x, and G_a is the Grashof number based on the fluid's absorption coefficient a.

Substituting Eqs. (5) and (6) into Eqs. (1) through (4), and performing the necessary mathematical operations, results in the following equations:

$$F''' + 4FF'' - 3F'^2 - \theta + 4\xi(GF'' - F'G') - 25\xi^{1/2}\,\text{Da}^{-1}F' - 5\xi^{5/4}\Gamma F'^2 = 0 \tag{7}$$

$$\theta'' + \text{Pr}(4F\theta' - F'\theta) - 4\xi\,\text{Pr}(F'H - \theta'G) - 5\xi^{1/4}\exp(-5\xi^{1/4}\eta) = 0 \tag{8}$$

where $\text{Da}^{-1} = 1/(Ka^2)$, $\Gamma = CG_a^5/a$, and $\text{Pr} = \rho\nu c/k_e$ are the inverse Darcy number, the dimensionless porous medium inertia coefficient, and the effective Prandtl number, respectively. In the quasi-similar Eqs. (7) and (8), a prime denotes ordinary differentiation with respect to η, and G and H are the first derivatives of F and θ with respect to ξ, respectively.

The transformed boundary and matching conditions can be shown to be

$$F(\xi, 0) = 0, \quad F'(\xi, 0) = 0, \quad \theta'(\xi, 0) = 5\alpha\xi^{1/4}\theta(\xi, 0)$$

$$F'(\xi, \infty) = 0, \quad \theta(\xi, \infty) = 0,$$

$$\theta(0, \eta) = 0, \quad F(0, \eta) = 0 \tag{9a–g}$$

where $\alpha = U/(k_e a)$ is the heat transfer loss coefficient. A typical value of α is 0.2 (corresponding to an absorbing fluid with a = 200 m^{-1} and a surrounding air moving at a speed of 5 m/s). Larger values of α can also be used for higher wind velocities and/or lower values of the absorption coefficient a.

Additional equations governing G and H are needed to render the problem complete, as is done by the local nonsimilarity technique (Sparrow and Yu, 1971). These are obtained by dif-

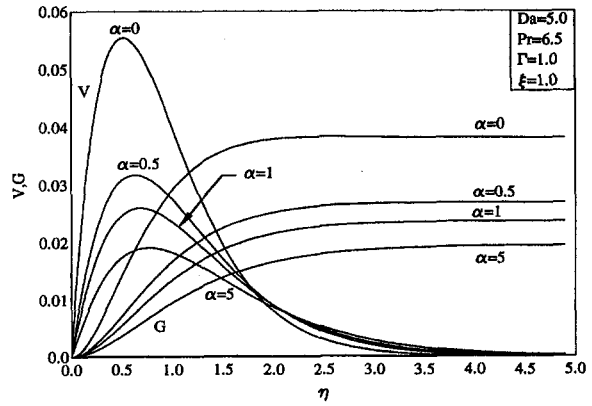

Fig. 4 Effects of α on tangential and normal velocity profiles

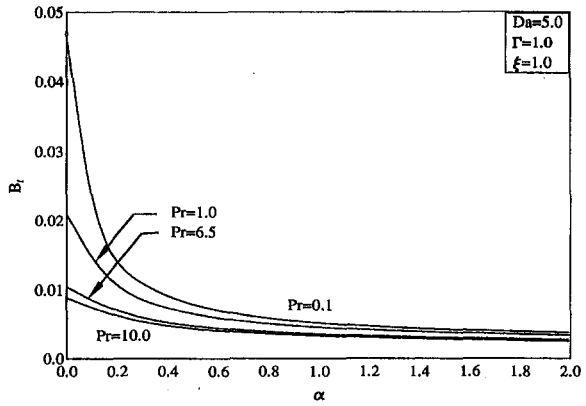

Fig. 6 Effects of Pr and α on boundary friction coefficient

ferentiating both Eqs. (7) and (8) with respect to ξ to respectively give

$$G''' + 4FG'' + 8GF'' - 10F'G' - H - 4\xi(G'^2 - GG'') - 25\xi^{1/2}\,\mathrm{Da}^{-1}G' - \tfrac{25}{2}\,\xi^{-1/2}\,\mathrm{Da}^{-1}F' - 10\xi^{5/4}\Gamma F'G' + \tfrac{25}{4}\,\xi^{1/4}\Gamma F'^2 = 0 \quad (10)$$

$$H'' + \mathrm{Pr}(8G\theta' + 4FH' - G'\theta - 5F'H) - 4\xi\,\mathrm{Pr}(G'H - GH') + \tfrac{5}{4}\,\xi^{-3/4}(1 - 5\xi^{1/4}\eta)\exp(-5\xi^{1/4}\eta) = 0. \quad (11)$$

Similarly, differentiating Eqs. (9) with respect to ξ yields the boundary and matching conditions for G and H as follows:

$$G(\xi, 0) = 0, \quad G'(\xi, 0) = 0,$$
$$H'(\xi, 0) - \tfrac{5}{4}\,\alpha\xi^{-3/4}\theta(\xi, 0) - 5\alpha\xi^{1/4}H(\xi, 0) = 0$$
$$G'(\xi, \infty) = 0, \quad H(\xi, \infty) = 0,$$
$$H(0, \eta) = 0, \quad G(0, \eta) = 0. \quad (12)$$

Equations (7) through (12) represent the governing equations for the problem under consideration. It should be mentioned that these ordinary differential equations are approximate since higher order ξ derivative terms are neglected, as required by the local similarity method. However, the exact equations are partial differential equations and can be easily solved numerically by a marching finite-difference technique, but the local similarity method herein is chosen so as to allow comparisons with the previously published work of Fathalah and Elsayed (1980). Also, note that setting $\Gamma = 0$ and letting $\mathrm{Da} \to \infty$, the equations reported by Fathalah and Elsayed (1980) are recovered.

Of special significance in free convection problems are the local boundary-friction coefficient and the Nusselt number. These physical parameters can be defined in dimensional form as

$$B_f^* = \frac{-\mu\partial^2\psi(x, 0)}{\partial y^2}, \quad \mathrm{Nu}_a = \frac{h}{k_e a},$$
$$h = \frac{q'' - U(T_w - T_\infty)}{T_{\max} - T_\infty} \quad (13a\text{–}c)$$

where μ is the fluid dynamic viscosity, T_w is the plate or wall temperature, $T_{\max}$ is the maximum local temperature, and h is the local heat transfer coefficient. Upon using Eqs. (6a–h), it can be shown that

$$B_f = \frac{B_f^*}{\rho\nu^2 G_x a^2} = -\frac{F''(0)}{25\xi^{1/2}},$$
$$\mathrm{Nu}_a = -\left(\frac{1}{5\xi^{1/4}\theta_{\max}} + \alpha\,\frac{\theta_w}{\theta_{\max}}\right). \quad (14a, b)$$

Results and Discussion

Equations (7) through (12) are nonlinear coupled ordinary differential equations and conditions that must be solved numerically since they exhibit no analytical solution. An implicit, iterative, tridiagonal finite-difference numerical method similar to that discussed by Blottner (1970) is devised for this purpose.

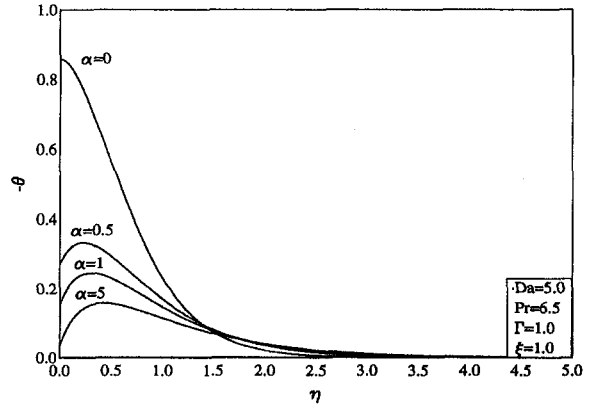

Fig. 5 Effects of α on temperature profiles

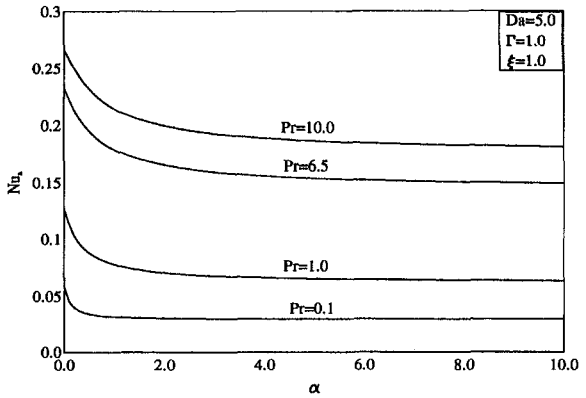

Fig. 7 Effects of Pr and α on Nusselt number

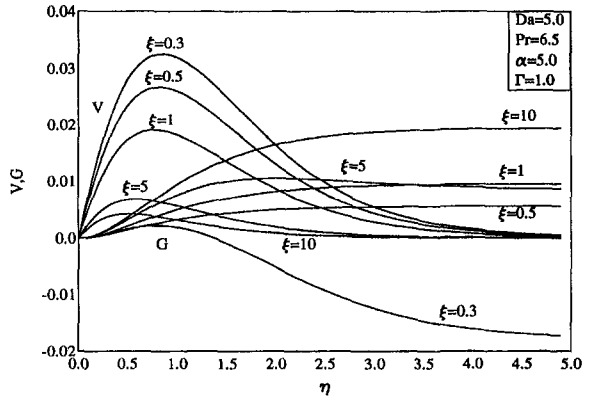

Fig. 8 Effects of ξ on tangential and normal velocity profiles

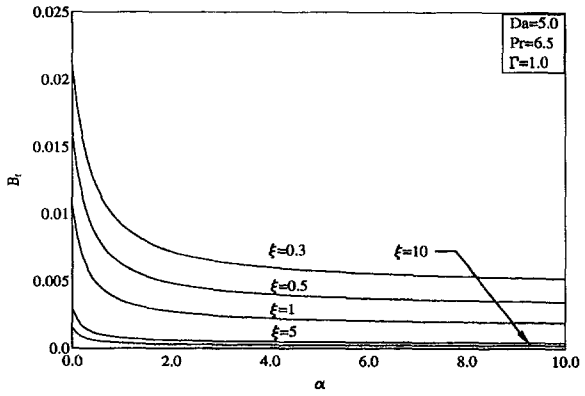

Fig. 10 Effects of ξ and α on boundary friction coefficient

The third-order differential equations are converted into second-order differential equations by making variable changes. Then, all second-order equations in η are discretized using three-point central difference quotients while first-order equations are discretized using the trapezoidal rule. With this, the differential equations are converted into a set of algebraic equations which are solved with iteration (to deal with the nonlinearities of the governing equations) by the Thomas' algorithm (see Blottner, 1970). Most changes in the dependent variables are expected to occur in the vicinity of the wall where viscous effects dominate. Far away from the wall the fluid adjusts to the ambient conditions and changes in the dependent variables are expected to be small. For this reason, variable step sizes in η are employed in the present work. The initial step size $\Delta\eta_1$ was set to 10^{-3} and the growth factor was set to 1.03. These values were arrived at after many numerical experimentations were performed to assess grid independence. A convergence criterion based on the relative difference between two successive iterations (set to 10^{-4} in the present work) was employed.

More details of the numerical solution and the procedure followed can be explained as follows:

Consider Eq. (7) governing the dimensionless stream function F. By defining

$$V = F' \tag{15}$$

Eq. (7) may be written (before the central-difference formulas are used) as

$$\pi_1 V'' + \pi_2 V' + \pi_3 V + \pi_4 = 0 \tag{16}$$

where

$$\pi_1 = 1, \quad \pi_2 = 4F + 4\xi G - (3 + 5\xi^{5/4}\Gamma)V$$

$$\pi_3 = -4\xi G' - 25\xi^{1/2}\,\mathrm{Da}^{-1}, \quad \pi_4 = -\theta. \tag{17a–d}$$

The boundary conditions for V are

$$V(0) = 0, \quad V(\eta_{\max}) = 0 \tag{18a, b}$$

where infinity is replaced by η_{max}, which is set to a maximum value of ten in the present work.

The coefficients π_1, π_2, π_3, and π_4 in the inner iteration step are evaluated using the solution from the previous iteration step. Equation (16) is then converted into tridiagonal finite-difference algebraic equations which can be solved by the Thomas' algorithm.

Equation (15) can be integrated to give

$$F_{n+1} = F_n + \frac{(V_{n+1} + V_n)\Delta\eta_n}{2} \tag{19}$$

where n corresponds to the nth point along the η direction.

The boundary condition for F is

$$F(0) = 0. \tag{20}$$

The same procedure can be applied to solve Eqs. (8), (10), and (11). Many numerical results were obtained throughout the course of this work. A representative set is reported below in Figs. (2) through (19).

Figures 2 and 3 show typical profiles for the fluid tangential velocity V, normal velocity G, and temperature θ along the vertical plate for various values of the Prandtl number Pr. Increases in the Prandtl number have a tendency to decrease both the tangential velocity and temperature and to confine them to

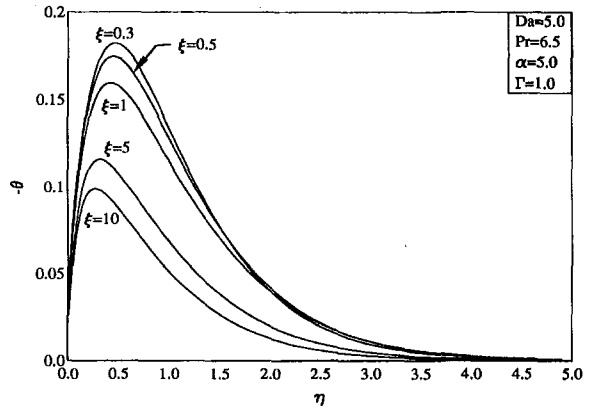

Fig. 9 Effects of ξ on temperature profiles

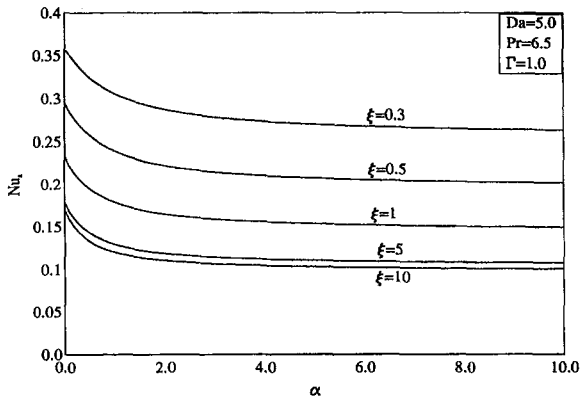

Fig. 11 Effects of ξ and α on Nusselt number

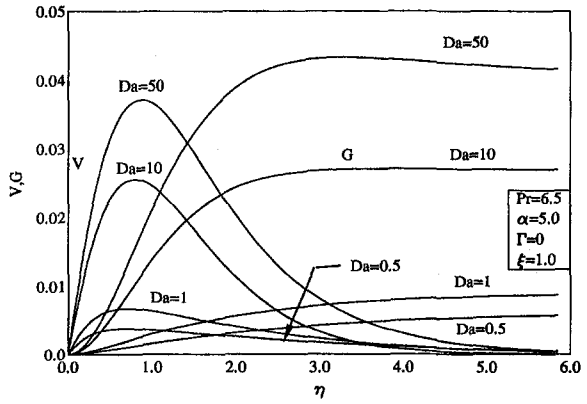

Fig. 12 Effects of Da on tangential and normal velocity profiles

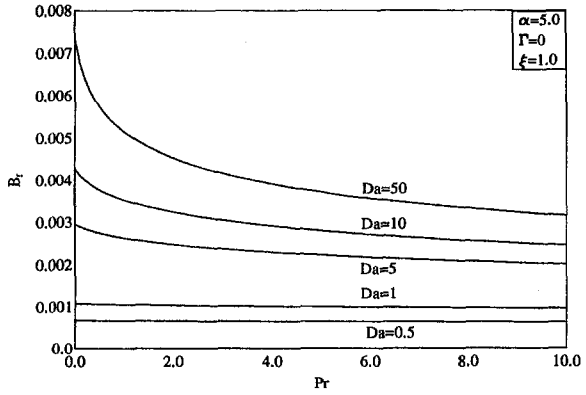

Fig. 14 Effects of Da and Pr on boundary friction coefficient

an increasingly smaller region closer to the vertical plate. In addition, the normal velocity of the fluid decreases as a result of increasing Pr. These behaviors are clearly depicted in Figs. 2 and 3. It is also seen from Fig. 3 that the maximum temperature occurs in the fluid away from the plate surface. This is because the incident solar radiations are absorbed by the absorbing fluid which in turn heats up the ideally transparent plate. This operation is believed to enhance solar collection by direct absorption in which heat losses are reduced as a result of lower plate temperatures.

Figures 4 and 5 show the influence of the heat transfer loss coefficient to the surrounding α on the tangential and normal velocity and temperature profiles, respectively. As the heat transfer loss to the surroundings increases, the absorbing fluid in the porous medium tends to slow down and its temperature tends to decrease. This is evident from the decreases in V, G, and θ as α increases (shown in Figs. 4 and 5). It can be seen from Fig. 5 that for $\alpha = 0$ (no heat loss to the surroundings) the maximum temperature occurs at the plate surface, which is consistent with results obtained for nonconvective boundary conditions.

Figures 6 and 7 present the boundary friction, B_f, and the Nusselt number, Nu_a, for various values of the effective Prandtl number, Pr, and the heat transfer loss coefficient to the surrounding α, respectively. It is observed from these figures that B_f and Nu_a decrease and increase for fixed values of α as Pr increases. The lower values of B_f are due to the lower tangential velocities predicted by increasing Pr. However, the increase in the Nu_a value is due to the reductions of the maximum temperature (occurring for higher values of Pr) since it is inversely proportional to it (see definition of Nu_a). Increases in the loss coefficient α have the same effect on the tangential velocity and temperature as that of Pr. Namely, it causes V and θ to decrease. This results in reductions in the values of both B_f and Nu_a as α increases. These behaviors are evident from Figs. 6 and 7, respectively.

Figures 8 through 11 illustrate the influence of the axial or tangential distance ξ on the flow and heat transfer parameters of the problem under consideration. Figures 8 and 9 present the profiles of the fluid tangential and normal velocity components, and the temperature profiles at different values of ξ (for Pr = 6.5 and $\alpha = 5$, corresponding to water at high wind velocities), respectively. Higher peaks in the values of the tangential velocity of the absorbing fluid V are observed at small values of ξ. This is related to the thickness of the fluid layer adjacent to the plate which is larger at lower values of ξ. It is also observed that a back-flow condition exists in the fluid's normal velocity component G for $\xi = 0.3$. This type of flow reversal behavior has been reported and discussed by Gebhart et al. (1988, p. 174). As ξ increases, the tangential velocity decreases while the normal velocity increases causing a slower net motion up the porous medium adjacent to the plate. The temperature distribution of the absorbing fluid also shows that higher peaks in the temperature occur for small values of ξ and these peak values decrease as ξ increases. Again, the maximum temperature does not occur at the plate surface as is the case of nonabsorbing fluids.

Figures 10 and 11 depict the changes of the boundary friction coefficient, B_f, and the Nusselt number, Nu_a, as a result of changing both α and ξ, respectively. As expected, higher tangential velocities at small values of ξ lead to higher boundary frictions, and as ξ increases, V decreases which results in increased reductions in B_f. This is evident from Fig. 10. Looking at the definition of Nu_a, it can be seen that Nu_a is inversely proportional to ξ for fixed values of α. Thus, an increase in the

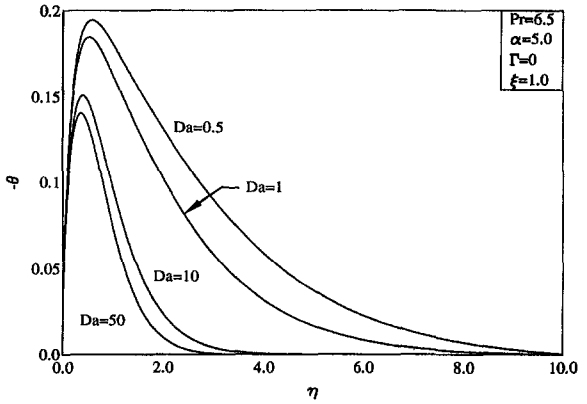

Fig. 13 Effects of Da on temperature profiles

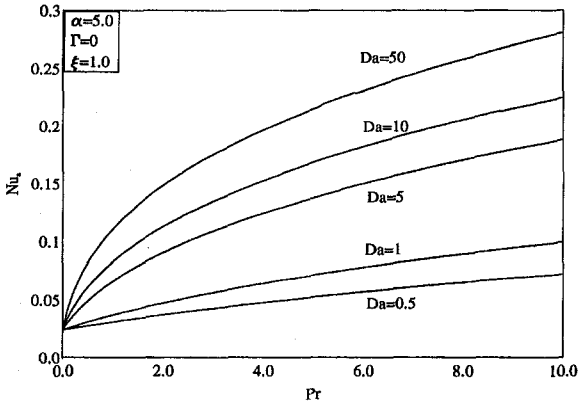

Fig. 15 Effects of Da and Pr on Nusselt number

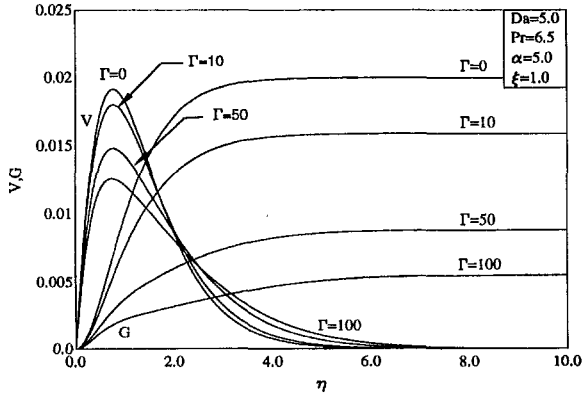

Fig. 16 Effects of Γ on tangential and normal velocity profiles

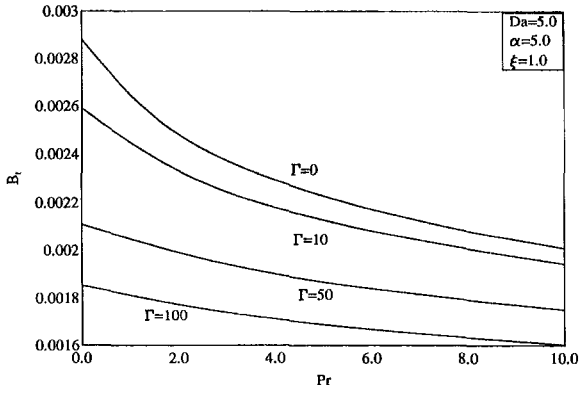

Fig. 18 Effects of Γ and Pr on boundary friction coefficient

values of ξ has the effect of reducing the Nusselt number. This behavior is clearly seen in Fig. 11.

Figures 12 through 15 elucidate the influence of the presence of the uniform porous medium on the flow and heat transfer through the Darcy number Da. The results in these figures are obtained for slow flow ($\Gamma = 0$) in order to evaluate the relative effect of Da alone. Figures 12 and 13 present the profiles for V, G, and θ for various values of Da. It should be noted that large values of Da correspond to high porosity porous medium, and the limit $Da \to \infty$ corresponds to the case of no porous medium present. Obviously, a high porosity porous medium exerts less resistance to flow. This causes higher tangential and normal fluid velocities, and these velocities decrease as the porous medium gets tighter (as Da decreases). This is clearly shown in Fig. 12. However, the presence of the porous medium (smaller values of Da) has the tendency to increase the fluid temperature. This is due to the increased fluid restriction resulting from decreasing the porosity of the porous medium. This behavior is evident from Fig. 13.

Figures 14 and 15 show the influence of both Da and Pr on B_f and Nu_a, respectively. As mentioned before, increases in Pr cause decreases in B_f and increases in Nu_a, for a relatively open porous medium. The slowing of the absorbing fluid as a result of decreasing the Darcy number, Da, has the direct effect on decreasing the wall or boundary friction as shown in Fig. 14. It is also seen that for small porosity medium, specifically for $Da = 0.5$ and $Da = 1.0$, B_f is constant for any value of Pr. It is also evident from Fig. 15 that increases in the values of Da (that is, increases in the porosity of the medium) cause increases in the Nusselt number at any fixed value of Pr. This is because Nu_a is inversely proportional to θ_{max} which decreases as Da increases.

The influence of the porous medium inertia coefficient Γ on the flow and heat transfer parameters is the same as that of the inverse Darcy number Da^{-1} since it also represents resistance to flow. Namely, as Γ increases, V, G, and B_f decrease while θ and Nu_a increase and decrease, respectively. These behaviors are depicted in Figs. 16 through 19.

It should be mentioned that for $\Gamma = 0$ and as $Da \to \infty$, the results reported by Fathalah and Elsayed (1980) are recovered. This comparison serves as a check on the numerical procedure. No comparisons with experimental data were performed due to lack of such data at present.

Conclusion

Natural convection flow of an absorbing fluid up a uniform porous medium supported by a semi-infinite, ideally transparent, vertical flat plate due to solar radiation is considered. Boundary-layer equations are derived using the usual Boussinesq approximation and accounting for applied incident radiation flux. A convection type boundary condition is used at the plate surface. These equations exhibit no similarity solution. However, the local similarity method is employed for the solution of the present problem so as to allow comparisons with previously published work. The resulting approximate nonlinear ordinary differential equations are solved numerically by a standard implicit iterative finite-difference method. Graphical results for the velocity and temperature fields, as well as the boundary friction and Nusselt number, are presented and discussed. It was found that increases in any of the following: effective Prandtl number, heat transfer loss coefficient, tangential distance along the plate, inverse Darcy number, and the porous medium inertia coefficient caused reductions in the boundary friction coefficient. However, the Nusselt number based on the absorbing fluid coefficient was increased as the Prandtl number

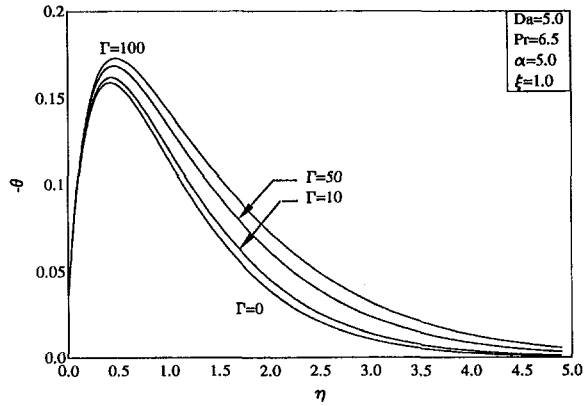

Fig. 17 Effects of Γ on temperature profiles

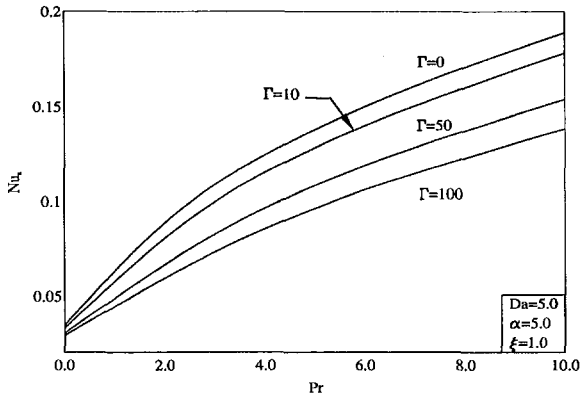

Fig. 19 Effects of Γ and Pr on Nusselt number

increased, and reductions were observed as a result of increasing any of the following: heat transfer loss coefficient, tangential distance, inverse Darcy number, and the medium inertia coefficient. In addition, a flow reversal condition was predicted for water with high heat transfer loss coefficient in the presence of a porous medium. Comparison with previously published work was performed and the results were found to be in excellent agreement. It is hoped that the present work will serve as a stimulus for experimental work which appears to be lacking at present.

References

Blottner, F., 1970, "Finite Difference Methods of Solutions of the Boundary-Layer Equations," *AIAA Journal,* Vol. 8, 193–205.

Chen, C., and Lin, C., 1995, "Natural Convection From an Isothermal Vertical Surface Embedded in a Thermally Stratified High-Porosity Medium," *International Journal of Engineering Science,* Vol. 33, 131–138.

Chen, C. K., Hung, C. I., and Horng, H. C., 1989, "Transient Natural Convection on a Vertical Flat Plate Embedded in a High-Porosity Medium," ASME JOURNAL OF HEAT TRANSFER, Vol. 109, 112–118.

Cheng, P., and Minkowycz, W. J., 1977, "Free Convection About a Vertical Flat Plate Embedded in a Porous Medium with Application to Heat Transfer From a Dike," *Journal of Geophysical Research,* Vol. 82, 2040–2044.

Cooper, P. I., 1972, "Some Factors Affecting the Absorption of Solar Radiation in Solar Stills," *Solar Energy,* Vol. 13, 373–381.

Elsayed, M. M., and Fathalah, K. A., 1979, "Temperature Distribution in a Direct Solar Heater," presented at the 72nd Annual Meeting of AIChE, Paper No. P–7d.

Evans, G. H., and Plumb, O. A., 1978, "Natural Convection From a Vertical Isothermal Surface Embedded in a Saturated Porous Medium," ASME Paper No. 78-HT-55.

Fathalah, K. A., and Elsayed, M. M., 1980, "Natural Convection Due to Solar Radiation Over a Non-Absorbing Plate With and Without Heat Losses," *International Journal of Heat & Fluid Flow,* Vol. 2, 41–45.

Gebhart, B., Jaluria, Y., Mahajan, R. L., and Sammakia, B., 1988, *Buoyancy-Induced Flows and Transport,* Hemisphere Publishing Corporation, New York, p. 914.

Hassan, K., and Mohamed, S., 1970, "Natural Convection From Isothermal Flat Surfaces," *International Journal of Heat and Mass Transfer,* Vol. 13, 1873–1886.

Hong, J., Yamada, Y., and Tien, C. L., 1987, "Effect of Non-Darcian and Nonuniform Porosity on Vertical-Plate Natural Convection in Porous Media," ASME JOURNAL OF HEAT TRANSFER, 109, 356–362.

Kierkus, W. T., 1968, "An Analysis of Laminar Free Convection Flow and Heat Transfer About an Inclined Isothermal Flat Plates," *International Journal of Heat and Mass Transfer,* Vol. 11, 241–253.

Kim, S. J., and Vafai, K., 1989, "Analysis of Natural Convection About a Vertical Plate Embedded in a Porous Medium," *International Journal of Heat Mass Transfer,* Vol. 32, 665–677.

Nakayama, A., Kokudai, T., and Koyama, H., 1990, "Non-Darcy Boundary Layer Flow and Forced Convective Heat Transfer Over a Flat Plate in a Fluid-Saturated Porous Medium," ASME JOURNAL OF HEAT TRANSFER, Vol. 112, 157–162.

Plumb, O. A., and Huenefeld, J. C., 1981, "Non-Darcy Natural Convection from Heated Surfaces in Saturated Porous Media," *International Journal of Heat Mass Transfer,* Vol. 24, 765–768.

Siegel, R., and Howell, J. R., 1981, *Thermal Radiation Heat Transfer,* Hemisphere Publishing Corporation, Washington, D.C.

Singh, P., and Tewari, K., 1993, "Non-Darcy Free Convection from Vertical Surfaces in Thermally Stratified Porous Media," *International Journal of Engineering Science,* Vol. 31, 1233–1242.

Sparrow, E. M., and Gregg, J. L., 1956, "Laminar Free Convection from a Vertical Plate With Uniform Surface Heat Flux," *Transfer ASME,* Vol. 78, p. 435.

Sparrow, E. M., and Yu, H. S., 1971, "Local Non-Similarity Thermal Boundary-Layer Solutions," ASME JOURNAL OF HEAT TRANSFER, Vol. 93, No. 4, 328–334.

Vafai, K., Ettefagh, J., 1988, "Analysis of the Radiative and Conductive Heat Transfer Characteristics of a Waste Package Canister," ASME JOURNAL OF HEAT TRANSFER, Vol. 110, 1011–1014.

Vafai, K., and Tien, C. L., 1982, "Boundary and Inertia Effects on Convective Mass Transfer in Porous Media," *International Journal of Heat Mass Transfer,* Vol. 25, 1183–1190.

Vafai, K., and Tien, C. L., 1981, "Boundary and Inertia Effects on Flow and Heat Transfer in Porous Media," *International Journal of Heat Mass Transfer,* Vol. 24, 195–203.